http://dx.doi.org/10.21611/qirt.1994.026

Steady and unsteady wall heat transfer mapping by active infrared thermography at the mean aerodynamic reattachment point behind a backward-facing step

By DUMOULIN J., REULET P., GRENIER P., PLAZANET M. and MILLAN P.

CERT - ONERA / DERMES, 2 Avenue Edouard Belin BP 4025, 31055 TOULOUSE Cedex, FRANCE

Abstract

Knowledge of the thermal behaviour of materials submitted to turbulent flows, is essential in many industrial problems, in particular when designing combustion chambers. So, experimental work is needed to gain a physical understanding of the steady and unsteady wall heat transfer. CERT - ONERA / DERMES has built an experimental method, with the financial support of DRET, in order to characterise the intensity and distribution of heat transfer coefficient (Hcv), around the mean aerodynamic reattachment point behind a backward-facing step. The Infrared Thermography, coupled with anemometric and pressure measurements allows us to build-up mean wall laws required for numerical simulations. The synchronization of measurements is exploited to show the possibility of building instantaneous wall heat transfer laws. A first analysis of unsteady results is proposed for an inlet velocity of 12 m/s, and compared to tomographic visualisations.

Nomenclature

a	Thermal diffusivity
Cp	Specific heat
e	Thickness
h	Heat transfer coefficient
H	Step height
U0	Inlet velocity
Xmax	Maximum heat transfer abscissa
Xr	Aerodynamical reattachment point abscissa

Greek Symbols

λ	Heat conductivity
σ	Stefan constant
ε	Hemispherical emissivity in the 8-12 μm band
φ	Heat flux density
ρ	Density
ν	Kinematic viscosity

Adimensional Numbers

Nu	Nusselt number
Re	Reynolds number
Pr	Prandtl number
Bi	Biot number

Subscripts

air	Air
aw	Adiabatic wall
f	Treated foil
cv	Forced convection
ray	Radiation
roof	Insulating lump in "Roofmate"

Short scripts

ThIR	Infrared Thermography
Hcv	Heat transfer coefficient by convection

1. Introduction

In this paper, a "Thin film" technique coupled with Infrared Thermography has been developed to qualify the intensity of mean and unsteady wall heat transfer in the reattachment area induced by the flow behind a backward-facing step. Many publications have been made on that technique [1] [2], but the originality of the present work is that the thin foil used has undergone a chemical conversion coating. So, thermophysical properties are unchanged and unsteady quantitative measurement can be realised at low frequency (less than 20 Hz). The direct thermal modelling of that specific surface (treated foil) is presented here with the corrections linked to the infrared system used. Then, the mean flow behind the backward-facing step is presented and analysed. The coupling of infrared measurement with velocity, fluctuating pressure and flow temperature measurements is realised. A correlation for the mean heat transfer in the aerodynamical reattachment zone for the testing bench of DERMES is then proposed. The use of tomographic visualisations allows us to develop a first analysis of the unsteady wall heat transfer and to conclude about the efficiency of classical frequencies analysis tools. Finally, comparisons are made between mean and unsteady measurements by using average values.

2. Measurements methodology

In order to determine the heat transfer coefficient versus time, an experimental tool has been developed. It consists in a specific surface, sensible to aerothermic fluctuations of the

The colour plates of this article are on page X at the end of the book.

http://dx.doi.org/10.21611/qirt.1994.026

flow. This surface is a treated foil tightened on an insulating stand and heated by Joule effect. It has to respect the following criteria :

•Thin body :

$$Bi = \frac{(h_{cv}(x,y,t) + h_{ray})\, e_{cl}}{\lambda_{cl}} < 0.1 \Rightarrow T(x,y,z,t) \approx T(x,y,t) \quad (1)$$

This thermal criteria allows us to assume that the temperature is constant in the thickness of the treated foil. The characteristic diffusion time by conduction, in the three dimensions of space, should be lower than the measurement sampling time. So, the steady state hypothesis during the measurement will be true [3].

• Small thermal inertia :

The characteristic convection time constant $\tau = \rho Ce / h$ must be as small as possible to allow the detection of the surface temperature oscillations by the ThIR. Furthermore, τ must be greater than the measurement sampling time to detect the temperature variations induced by the forced convection.

• Insulated back surface :

It allows us to assume that no heat flux dissipation or absorption is lost by the insulated stand during the experiment.

The effusivity ratio between the treated foil and the insulating lump is such that the contact temperature at the interface will be dictated by the treated foil :

$$\frac{\sqrt{\lambda_f \rho_f C_f}}{\sqrt{\lambda_{roof} \rho_{roof} C_{roof}}} \approx 232 \quad (2)$$

A simplified study of the influence of the insulated stand can be made by taking into account sinusoidal variations of its surface temperature : $T(0,t) = T0 + A\cos\omega t$. The behaviour of the heat flux at the surface of the insulated lump can be written as : $\varphi(0,t) = A\sqrt{\lambda\rho C\omega}\cos\left(\omega t + \frac{\pi}{4}\right)$. In the case of the impingement of a pulsed air jet on a flat plate, which has been chosen as a validation method, published in [4] [5], an error of about 10 % is done on the value of heat flux given by Joule effect to the treated foil. This error is located in the maximum heat exchange area and due to the difference of temperature in between the surface and the adiabatic wall (equation [4]), the final error on the htc value is insignificant. Some reference values in steady state can be found in Goldstein and al.'s publication [6] and the aerodynamic of the impingement has been well studied by Ozedmïr and al [7].

The energy balance equation for the sensible surface, with the hypothesis detailed forward, can be written :

$$q + \varphi_{acc} + \varphi_{cd} + \varphi_{ray} + \varphi_{cv} = 0 \quad (3)$$

It takes into account different kinds of heat flux inside the treated foil and surface conditions which are convection and radiation. Then the value versus time of the local heat transfer coefficient by convection is deduced from the knowledge of the evolution of the surface temperature and the wall adiabatic temperature corrected during the measurement :

$T_{ref}(x,y,t) = T_{aw}(x,y,t) + \Delta T_{aw}(x,y,t)$.

The discretized expression of the time dependent heat exchange coefficient, in the case of the sensible surface submitted to the flow and heated by Joule effect, deduced from the modelisation is written as :

$$h_{cv}(x,y,t) = \frac{\frac{U.i}{S_{cl}} - \rho_{cl} C_{cl} e_{cl} \frac{T(x,y,t+\Delta t) - T(x,y,t-\Delta t)}{2\Delta t}}{(T(x,y,t) - T_{ref}(x,y,t))} - \frac{\varepsilon_{cl}\sigma(T^4(x,y,t) - T_{ref}^4(x,y,t))}{(T(x,y,t) - T_{ref}(x,y,t))} \quad (4)$$

$$+ \frac{e_{cl}\lambda_{cl}\left(\frac{T(x+\Delta x,y,t) + T(x-\Delta x,y,t) - 2T(x,y,t)}{\Delta x^2}\right) + \left(\frac{T(x,y+\Delta y,t) + T(x,y-\Delta y,t) - 2T(x,y,t)}{\Delta y^2}\right)}{(T(x,y,t) - T_{ref}(x,y,t))}$$

http://dx.doi.org/10.21611/qirt.1994.026

In equation [4], appears the wall temperature which is measured by Infrared Themography and the sensible surface emissivity (treated foil). These two points are developed in the next paragraph.

3. Experimental means

To study the heat transfer coefficient at the wall, two kinds of experimental means have been used. First, those which allow us to characterise and to gain a physical understanding of the flow in the field and at the wall :

- Laser velocimetry
- Hot wire anemometry
- Wall pressure fluctuation measurements
- Tomographic visualisations

And others, which allow us to characterise the thermal behaviour of the wall and the flow :

- Infrared thermography
- Temperature measurements by Thermocouples or cold wire placed on the testing bench

Those two kinds of experimental means have been the subject of many publications [8], [9], [10], [11] and [12]. In that paper we will briefly present the Infrared Thermography system and the new software developed at DERMES. Furthermore, it will help us to explain the choice of a chemical coating conversion for the thin metallic foil which constitutes the sensible surface mounted on the wall (*figure* 1).

The infrared system used is made of :

- AGEMA 880LWB : long wave (8-12 μm) infrared scanner
- CATS E 2.00 : acquisition software
- TIC 8000 : acquisition hardware (8 bits digitization)
- 2 ways for the acquisition :
  - ⇒ image (maximum sampling frequency 6.25 Hz) for steady state measurements
  - ⇒ line (maximum sampling frequency 2500 Hz) for unsteady state measurements

To obtain a good measurement, the characteristics of the infrared system used have to watch a surface with an emissivity as big as possible. In general, a thin layer of paint is associated with the surface, which raise considerably the thermal inertia and begin unfavourable to the unsteady measurements. As, according to the thermal modelisation, our aim is to keep the thermal inertia of the treated foil as small as possible, a chemical conversion coating has been undergone on it. After treatment the hemispherical emissivity is 0.64 without modification of the other thermophysical properties and the final thickness is 10 μm.

Then, the evolution of surface temperatures measured by ThIR are exploited by using the software developed at DERMES [4] [5]. That one makes corrections on the measurement by taking into account the characteristics of the Infrared system used and gives the value of the unsteady Hcv by using directly the finite difference equation presented in the previous paragraph (equation [4]).

4. Application to the flow behind a backward facing step

The measurement method of the unsteady heat transfer coefficient developed, is used to study the reattachment point of the flow behind a backward facing step. Results are compared to tomographic laser visualisations of the flow and to anemometric and pressure measurements.

4.1.Experimental set-up and general aerodynamical characteristics

The experimental wind tunnel used is of Eiffel type equipped with a plenum chamber and a convergent in order to get a regular velocity profile at the entry of the step (see *figure* 2). At the end of the test section, a divergent connects it to the wind tunnel. The set-up has been dynamically and acoustically characterised, and the air flow in the test section (at ambient temperature) can be considered as a two dimensional one in mean values. Nonetheless,

http://dx.doi.org/10.21611/qirt.1994.026

transverse tomographic visualisations and laser anemometry show some perturbations occurring in this transverse direction for high velocities.

However, the geometric characteristics of the loop, should generate a two dimensional flow (Bradshaw [13]). These are the following :

- Aspect ratio : $\frac{Z}{H} = 10$ with $H = 50mm$
- Expansion ratio : $Er = 1.33$
- Velocity range : $2.10^4 \leq Re_H \leq 8.10^4$

We also perform hot wire and laser measurements which allow us to characterise the aerodynamic of the flow, in particular the regime of the boundary layer :

- Regime of the boundary layer at the nose of the step :
  - $\Rightarrow$ Laminar for : $Uo \leq 13$ m/s
  - $\Rightarrow$ Turbulent for : 17 m/s $\leq Uo$
- Regime of the reattachment point is always turbulent
- The average position of the reattachment point is 6H

That aerodynamical study is not the main object of that paper, but the full experiment and its analysis can be found in P. Zaffalon's report [14].

The set-up of the Infrared thermography is shown on *figure* 2. That set-up is done in order to be able to watch the sensible surface through an Infrared window. The sensible surface is mounted on the aerodynamical reattachment area. So, the characterisation and the proposed correlation presented in that paper will just concern that part of the wall heat transfer. Some tomographic visualisations are used to raise our physical understanding of the phenomenon induced at wall by the flow around the reattachment point (Xr).

4.2.Mean heat transfer analysis

At first, the infrared temperature field is made by averaging 250 images in acquisition, however velocities and wall fluctuating pressure measurements are made at the same time. After that, a heat transfer coefficient map is computed, an example of temperature and Hcv map is shown on *figure* 3. It can be observed that, for low velocity, the bidimensionality of the heat transfer coefficient is saved. On such a map, we determine the position of the maximum for heat exchange at the wall (X_{max}). *Figure* 4 shows the evolution of X_{max} and X_r versus different inlet velocities U_0. X_{max} seems to be a growing function of U_o, when X_r is decreasing. Moreover, we perform a correlation for X_{max} versus U_0, based on our experimental results. The X_{max} change of location from X_r has been yet observed by Sparrow [15] and Vogel [16], and $X_{max}=X_r$ only constitutes a particular case. So, all the measurements realised allow us to propose a correlation for the heat transfer in the mean aerodynamical reattachment area. That correlation (system [5]) is built by using the localisation of the maximum of heat exchange. Furthermore, as the distribution of heat transfer is dissymetric between upstream and downstream X_{max}, we have divided it in two parts :

$$\begin{cases} X_{max} = 272 + 0.01 \cdot \left(U_0 - 13.0\right)^{3.43} \text{ with } X_{max} \text{ in mm and } U_0 \text{ in m/s} \\ Nu_H^{max} = 0.376 \cdot Pr^{1/3} \cdot Re_H^{0.62} \\ X < X_{max} : Nu_H(X) = Nu_H^{max} \cdot Exp\left[-0.441 \cdot \left(\frac{X - X_{max}}{X_{max}}\right)^{1.115}\right] \\ X > X_{max} : Nu_H(X) = Nu_H^{max} \cdot Exp\left[-1.047 \cdot \left(\frac{X - X_{max}}{X_{max}}\right)^{1.414}\right] \end{cases} \quad (5)$$

It is important to remark here that to generalise this correlation, experiments should be done for different expansion ratio and inlet boundary layer thickness.

http://dx.doi.org/10.21611/qirt.1994.026

Comparison with literature is difficult because, as we know, just Shishov and al. [17] propose a correlation for the value of maximum heat transfer coefficient in that kind of sudden expansion geometry. The other results available in literature do not match with the experimental conditions of the testing bench of DERMES.

4.3. Tomographic visualisations analysis

All the tomographic visualisations made for different Reynolds show the persistence of some phenomenon but the analysis difficulty increases with the inlet velocity.

The *figure* 5 presents tomographic visualisations of the flow for an inlet velocity of 10.4 m/s and an image sampling frequency of 1000 Hz. The nose of the backward-facing step is on the left of the picture.

On that *figure* we can observe the presence of coherent structures generated by the velocity gradient inside the shear layer. These coherent structures behave as they were in a mixing layer (Brown and Roshko [18]). They are convected by the mean movement with a velocity near U_0 / 2. The interaction between this high energetical swirl and the recirculating zone increases the pairing phenomenon. A basic eye analysis of the visualisation acquired close to the nozzle of the step allows the identification of the swirling detaching frequency, the pairing frequency and the return frequency. The location of the two first phenomena is also made and summed up in the board below :

Results of the tomographic visualisation quantitative analysis				
U_0 [m/s]	6.7	10.4	12.3	20
Detaching frequency in Hz	100 to 120	260 to 300	330 to 350	400 to 500
Adimensional location of the detaching from the nozzle of the step (in X/H)	1.1 to 1.35	0.55 to 0.75	0.7 to 1.3	0.58 to 0.92
Pairing frequency in Hz	50 to 60	160	indistinguishable	indistinguishable
Adimensional location of the pairing from the nozzle of the step (in X/H)	2.5	1.1	indistinguishable	indistinguishable
Return frequency in Hz	2.5 to 4	9 to 11	15 to 20	20 to 30

Furthermore, the visualisations realised in the aerodynamical reattachment zone seem to show the existence of a strong link between two phenomena :

- The recirculating zone draining
- The big structures impact at wall

Two phases can be identified :

- The draining seems to provoke the upstream sliding of the structures without interaction with the wall. It breaks also the swirling detaching.
- After the draining, one or more structures fully impact at wall which induce a new raise up in pressure in the recirculating zone.

These last remarks should be justified again by tomographic visualisations coupled with pressure measurements.

4.4.Unsteady heat transfer analysis

Figure 6 shows an Hcv profile along the time for an inlet velocity U0=12 m/s, the flow direction is presented on the left of the picture. The variations of X_r observed by tomographic visualisations appear also for the location of the maximum of heat transfer X_{max}. Sometimes, the difference between the mean value and the instantaneous value of the Hcv raise up to 40%.

http://dx.doi.org/10.21611/qirt.1994.026

On *figure* 7 two profiles are drawn. The first one, in black, is the distribution of the mean local value of Hcv obtained before (see paragraph 4-1) for an inlet velocity of 12 m/s. The second, in grey and for the same inlet velocity, is an average value of the profiles presented on *figure* 6. We can observe some local divergence in-between the two values because of the different period of averaging (the black is 40 s of averaging and the grey is 5 s of averaging). Another explanation is that in line mode the conduction correction works only in one direction (the flow direction). So according to the three dimensional behaviour of the turbulence at the reattachment point, this omission of the lateral conduction can induce some divergence. Nevertheless, this difference is less that ten percent of the mean value which respect the uncertainty of that experimental method.

Figure 8 shows three density power spectra of the unsteady Hcv located at $X= X_r$, $X=X_{max}$ and upstream X_{max}. The analysis of these spectra can just be made up to 20 Hz because, at that date, that frequency is the limitation of our method validation. The return frequency appears only for the point upstream Xmax around 10 Hz which is correlated with the visualisations analysis. Nevertheless, the maximum of energy appears around 50 Hz due to the amplification of the temperature noise measurements by the chosen direct modelisation.

So, one way to improve our understanding of the unsteady wall heat transfer induce by the variations of the flow is to develop a new treatment tool. This tool should be able to extract information delivered by ThIR and fluctuating pressure and velocity measurements acquired at the same time. To conclude, our unsteady heat transfer measurement method can be exploited to estimate the mean value of the convection velocities of the flow at wall by cross correlation between two points of the profiles.

Remark :

The fluctuation of X_{max} increases with U_0, which means that the turbulent agitation grows.

5. Conclusions

The qualification of the mean and unsteady wall heat transfer by the "thin film" method presented in that paper is done. The feasibility of coupling ThIR with velocity, fluctuating pressure and temperature measurements is demonstrated. Informations delivered by such a measurement set-up has been used to elaborate a correlation for the mean wall heat transfer as a function of the flow characteristics. The proposed correlation for the reattaching zone of a flow behind a backward-facing step is available for the testing bench of DERMES and its own flow characteristics. Nevertheless, the choice of X_{max} as a reference point to separate the distribution of the heat transfer could be generalized includind the sublayer thickness and state at the nose of the step and the height of that one. The local unsteady heat transfer coefficient shows some non negligible divergence with its mean value up to 40 %. Those phenomena could easily induce some local thermal loads inside combustion chamber. Nontheless, the first unsteady analysis shows that the classical frequency analysis is not efficient enough due to complexity of the frequencies present in the aerodynamic reattachment zone. A new analysis tool should be developed, a time-frequency one for example. Finally, this measurement method could be improved by performing the sensible surface (treated foil) and using an Infrared matricial scanner to include a two dimensional correction in time in the thermal modelisation.

REFERENCES

[1] ALIAGA (D.), KLEIN (J.), LAMB (P.) "*Heat transfer measurements on a ribbed surface at constant heat flux using infrared thermography*", Experimental Heat Transfer, vol 6, pp 17-34, 1993.

[2] CARDONE (G.), DI LEVA (O. M.) and CARLOMAGNO (G. M.) "*Heat transfer measurements and surface flow visualization of a backward facing step turbulent flow*", Experimental and numerical flow visualization, ASME winter annual meeting, 1993.

[3] BARDON (G. M.), "*Régimes thermiques instationnaires : Analyse physique de quelques comportements caractéristiques*", Colloque SFT 92, Mai 1992, Sophia-Antipolis.

http://dx.doi.org/10.21611/qirt.1994.026

[4] DUMOULIN (J.), MILLAN (P.), PLAZANET (M.), *"Steady and unsteady wall heat transfer mapping by active infrared thermography in perturbed aerodynamic situations"*, Experimental and numerical flow visualization, ASME winter annual meeting, 1993.

[5] DUMOULIN (J.), *"Méthodes de détermination, par thermographie infrarouge, des coefficients d'échange de chaleur moyens et instationnaires en aérodynamique perturbée"*, Thèse de l'Institut National des Sciences Appliquées de Toulouse, Mars 1994.

[6] GOLDSTEIN (R.J.), FRANCHETT (M.E.), *"Heat transfer from a flat surface to an oblique impinging jet"*, Transactions of the ASME, Journal of Heat Transfer, vol 110, pp 84-90, Février 1988.

[7] BEDII OZEDMIR (I.) and WHITELAW (J. H.), *"Impingement of an axisymmetric jet on unheated and heated flat plates "*, International Journal of Fluid Mechanics, vol 240, pp 503-532, 1992.

[8] "Anémométrie Doppler à laser", DANTEC, Cours LDA 3, Décembre 1986.

[9] MALARD (L.), *"Contribution à l'étude expérimentale des écoulements giratoires en conduite : influence*
l'Aéronautique et de l'Espace, Octobre 1993.

[10]AGEMA (INFARED SYSTEM), " *Manuel d'utilisation et document technique de la caméra 880 LWB*".

[11]GAUSSORGUES (G.), *"La thermographie infrarouge"*, TEC DOC Lavoisier, 1984.

[12]PAJANI (D.), *"Mesure par thermographie infrarouge"*, ADD, 1989.

[13]BRADSHAW (P.), DE BREDERODE (U.), *"Three dimensional flow in nominally two-dimensional separation bubles.Flow behind a rearward step "*, I.C. Aero-Report 72-19, 1972.

[14]ZAFFALON (P.), *"Contribution à l'étude aérodynamique d'un écoulement de type marche"*, Mémoire C.N.A.M., Spécialité : Aérodynamique, Juillet 1993.

[15]SPARROW (E.M.), KANG (S.S.), CHUCK (S.S.), *"Relation between the points of flow reattachment and maximum heat transfer for regions of flow*
transfer, vol 30, No 7, pp 1237-1246, 1987.

[16]VOGEL (J.C.) and EATON (J.K.)," *Combined heat tranfer and fluid dynamic measurements downstream of a backward-facing step"*, Transactions of the ASME, Journal of Heat Transfer, vol 107, pp 922-929, 1985.

[17]SHISHOV (E.V.), ROGANOV (P.S.), GRABARNIK (S.I.), ZABOLOTSKY (V.P.), *"Heat transfer in the recirculating region formed by a backward-facing step"*, International Journal of Heat and Mass transfer, vol 31, No 8, pp 1557-1562, 1988.

[18]BROWN (G.L.), ROSHKO (A.), *"On the density effects and large structure in two-dimensional mixing layers"*, Journal of Fluid Mechanics 64, pp. 775-816, 1974.

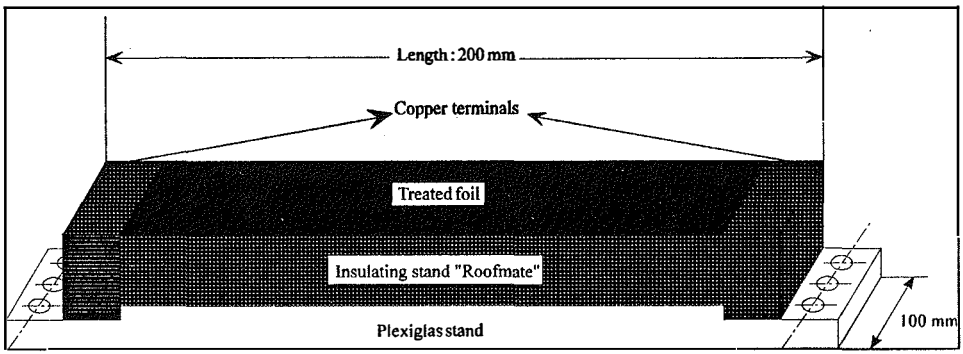

Figure 1 : Spatial arrangement of the sensible surface

http://dx.doi.org/10.21611/qirt.1994.026

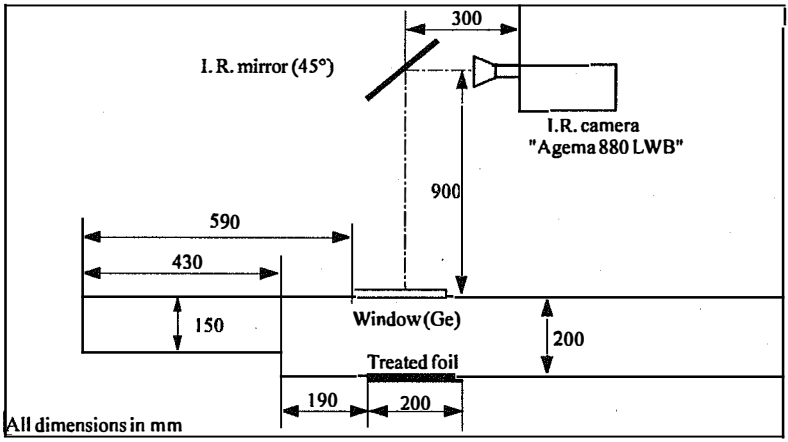

Figure 2 : Experimental set-up of the backward-facing step